THE JOURNAL OF PHYSICAL CHEMISTRY B

Article

pubs.acs.org/JPCB

Effects of Magnetic Field Cycle on the Polarization Transfer from Parahydrogen to Heteronuclei through Long-Range J-Couplings

Eleonora Cavallari, Carla Carrera, Tommaso Boi, Silvio Aime, and Francesca Reineri*

Department Molecular Biotechnology and Health Sciences, University of Torino, Via Nizza 52, Torino 10125, Italy

Supporting Information

ABSTRACT: Hyperpolarization of ^{13}C carboxylate signals of metabolically relevant molecules, such as acetate and pyruvate, was recently obtained by means of ParaHydrogen Induced Polarization by Side Arm Hydrogenation (PHIP-SAH). This method relies on functionalization of the carboxylic acid with an unsaturated alcohol (side arm), hydrogenation of the unsaturated alcohol using parahydrogen, and polarization transfer to the target ^{13}C signal. In this case, parahydrogen protons are added three to four bonds away from the target ^{13}C nucleus, while biologically relevant molecules had been hyperpolarized, using parahydrogen, through hydrogenation of an unsaturated bond adjacent to the target ^{13}C signal. The herein reported results show that the same polarization level can be obtained on the ^{13}C carboxylate signal of an ester by means of addition of parahydrogen to the acidic or to the alcoholic moiety and successive application of magnetic field cycle (MFC). Experimental results are supported by calculations that allow one to predict that, upon accurate control of magnetic field strength and speed of the passages, more than 20% polarization can be achieved on the ^{13}C-carboxylate resonance of the esters by means of side arm hydrogenation and MFC.

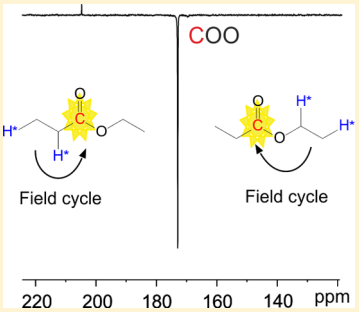

INTRODUCTION

Magnetic resonance (MR) spectroscopy and imaging are powerful tools for biomedical applications, albeit the intrinsic low sensitivity of these techniques still represents a limit to their possibilities. Hyperpolarization methods opened new perspectives to in vivo magnetic resonance allowing innovative investigations,[1−3] among which is the in vivo detection of metabolic processes in real time.[4−9] This was obtained through an increase of the MR signal of the target molecules by >10 000 times.[10] Then, since hyperpolarization is a transient state and signals tend to thermodynamic equilibrium, polarization of spins with long relaxation time and low background signal, such as nonprotonated ^{13}C or ^{15}N containing molecules,[10−12] is generally preferred for in vivo applications.

As far as in vivo metabolic studies are concerned, the dynamic nuclear polarization (DNP) technique played a major role, so far, since it allows one to obtain a ^{13}C-MR signal of biologically relevant molecules, among which pyruvate increase more than 10 000 times with respect to thermal equilibrium. Hyperpolarized pyruvate, once administered to living systems, allows a direct readout of cellular biochemical pathways; in particular, higher transformation into lactate is observed in diseased tissues and is used for cancer detection and staging.[13] Moreover, it was shown that this approach is particularly useful to monitor the therapeutic response to treatments.[14]

Parahydrogen induced polarization (PHIP)[15,16] is a route to hyperpolarization that does not suffer from high costs and technical constrains of the DNP methodology. PHIP relies on the addition of parahydrogen to unsaturated substrates, where the intrinsic spin order of parahydrogen is transformed into hyperpolarization of protons and heteronuclear signals. Some biologically relevant molecules have already been hyperpolarized by means of the PHIP method, and few of them have also been applied to in vivo studies.[11,17−20] The need for an unsaturated precursor of the target molecule, to which parahydrogen is added, strongly limited the application of PHIP for metabolic studies so far. It was recently demonstrated[21] that hyperpolarization of the ^{13}C carboxylate signal of molecules such as pyruvate and acetate, for which dehydrogenated precursors do not exist, can be obtained by means of the following steps: (i) functionalization of the carboxylate group with an unsaturated alcohol (called side arm); (ii) parahydrogen addition to the unsaturated alcoholic moiety; (iii) polarization transfer from parahydrogen spin order to the ^{13}C carboxylate signal; (iv) removal of the side arm by means of hydrolysis. It is worth mentioning that, even though hydrolysis is necessary to obtain the free acid, ethyl pyruvate[22] and ethyl succinate[19] were also used in vivo for biomedical studies. The reported method, called PHIP-SAH (PHIP by means of side arm hydrogenation), allows one to obtain ^{13}C-carboxylate hyperpolarization on biologically relevant molecules and considerably widens the applicability of hyperpolarization by means of parahydrogen.

In order to efficiently transfer hyperpolarization to heteronuclear signals, different methods were applied, relying on pulse sequences,[23−25] magnetic field cycling,[26,27] and, more recently, adiabatic passage through level anti crossing.[28] In molecules hydrogenated using parahydrogen, polarization

Received: June 29, 2015
Revised: July 10, 2015
Published: July 10, 2015

DOI: 10.1021/acs.jpcb.5b06222
J. Phys. Chem. B 2015, 119, 10035−10041

transfer to heteroatoms depends on the whole J coupling set between parahydrogen protons and heteronuclei. It was early shown[29,30] that the amount of polarization transferred to the ^{13}C resonance depends on the ratio between asymmetry of the proton-carbon J couplings ($\Delta J_{HX-H'X}$) and proton−proton J coupling ($J_{HH'}$). On this basis, polarization transfer to heteroatoms decreases when the involved J couplings are smaller than 1−2 Hz. More than 15−20% polarization was reported on ^{13}C nuclei placed two to three bonds away from the added parahydrogen protons,[11,18] that is, when the unsaturated group is adjacent to the ^{13}C nucleus.

The herein reported study addresses more in depth the issue of the polarization level that can be achieved on the ^{13}C carboxylate signal when parahydrogen is added to the alcoholic instead of the acid moiety of an ester, that is, on SAH derivatives.

EXPERIMENTAL METHODS

Ethyl acrylate (**1**) and vinyl propionate (**3**) were chosen as unsaturated substrates to carry out the experiments. Parahydrogen addition to both substrates leads to the same product ethyl-propionate (**2**) (scheme1).

Scheme 1. Hydrogenation of Ethyl Acrylate (1) and Vinyl Propionate (3) Leads to the Same Product Ethyl Propionate (2)

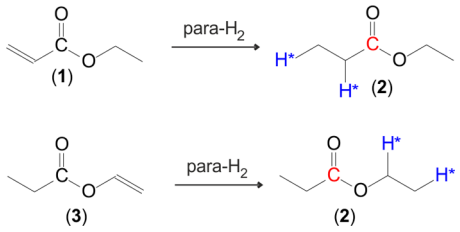

Hydrogenation reactions were carried out in NMR tubes, equipped with a Young valve, which were charged with 400 μL of an acetone-d_6 solution of the hydrogenation catalyst [RhCOD(ddpb)][BF_4] (7 mM). The catalyst was activated by hydrogenation of the coordinated diene, the substrate was added (50−80 mM), the solution was degassed by the freeze−thaw−pumping method, and the tube was pressurized with 6−7 bar of parahydrogen (92% enriched). In order to initiate the hydrogenation reaction, the tube was vigorously shaken for 5 s at earth's magnetic field (Figure 1a), and then, in the first series of experiments, the NMR tube was immediately placed in the MR spectrometer where a single scan ^{13}C NMR spectrum was acquired (Figure 1c).

In the second set of experiments, the magnetic field cycle was applied immediately after the hydrogenation with parahydrogen (Figure 1b). For this purpose, two concentric μ-metal cylinders were used to shield the laboratory's magnetic field. The NMR tube was dropped into the magnetic field shield (fast passage, nonadiabatic, approximately less than 1 s) and then, after a delay of about 2s into the shield, was slowly taken out (slow, adiabatic passage, about 5 s).

The hydrogenation catalyst [1,4-bis(diphenylphosphyno)-butane](1,5-cyclooctadiene)rhodium(I) tetrafluoroborate (98%, part number 341134) was bought from Sigma-Aldrich. Vinyl propionate and ethyl acrylate were synthesized as reported in the Supporting Information.

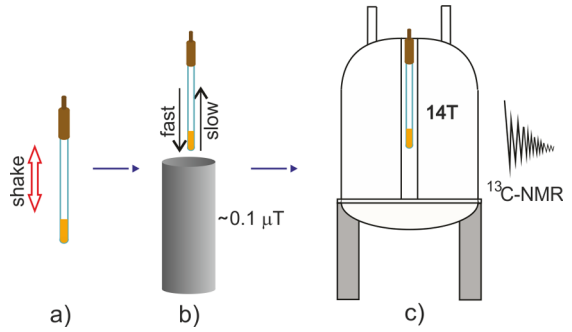

Figure 1. Schematic representation of the experimental procedure: (a) the NMR tube, charged with the hydrogenation mixture and pressurized with parahydrogen, is vigorously shaken (~5s); (b) the laboratory's magnetic field is shielded by μ-metal cylinders, and magnetic field cycle is carried out (fast passage: ~1s; slow passage ~5s); (c) the sample is placed in the NMR spectrometer, and a single scan ^{13}C NMR spectrum is acquired.

Hydrogen enriched in para isomer (92% enrichment) was obtained using a Bruker BPHG cryostat operating at 36K, supplied with normal hydrogen produced by a hydrogen generator (F-DGS hydrogen gas generator, serie WM-H2, purity 99.99%).

The NMR spectra were acquired using a 600 MHz Bruker Avance NMR spectrometer.

The two μ-metal cylinders (80% nickel, 15% iron, 5% molybdenum, traces of C, Si, and Mn, Meca-Magnetic, Amilly, France) were 300 mm height, 0.8 mm thick, 70 mm and 120 mm large, respectively.

THEORETICAL METHODS

The time evolution of the spin system during magnetic field cycling was described using the full density matrix approach. The whole process was divided into three steps: (1) parahydrogen addition to the substrate at earth's magnetic field, (2) nonadiabatic passage of the sample from earth's field to zero field, and (3) adiabatic remagnetization.

Step 1. Parahydrogen addition to the unsaturated substrate. This was considered as a sudden perturbation of the parahydrogen state, described by the density operator

$$\sigma_{para} = \frac{E}{4} - (I_x^A I_x^{A'} + I_y^A I_y^{A'} + I_z^A I_z^{A'}) \quad (1)$$

given by the Hamiltonian of the product molecule. Since protonated substrates were used, one parahydrogen proton was added to yield a methyl while the other gave a methylene group, therefore, the Hamiltonian, at earth's field, of the $A_3A'_2X$ spin system obtained from hydrogenation was

$$\mathcal{H}_{earth} = -\nu_H(\boldsymbol{I}_z^H + \boldsymbol{I}_z^{H'}) - \nu_C I_z^X + J_{AA'}[\boldsymbol{I}_z^H \boldsymbol{I}_z^{H'} + \boldsymbol{I}_x^H \boldsymbol{I}_x^{H'} + \boldsymbol{I}_y^H \boldsymbol{I}_y^{H'}] + J_{AX}(\hat{\boldsymbol{I}}_z^H \hat{I}_z^X) + J_{A'X}(\hat{\boldsymbol{I}}_z^{H'} \hat{I}_z^X) \quad (2)$$

where boldface operators refer to each subset of magnetically equivalent nuclei (see the Supporting Information). After reaction finishing, a new steady state was reached, similar to that previously reported,[31] as follows

$$\bar{\sigma}_{earth} = E/4 - I_z^H I_z^{H'} - \bar{a}_1^{earth}(\boldsymbol{I}_x^H \boldsymbol{I}_x^{H'} + \boldsymbol{I}_y^H \boldsymbol{I}_y^{H'}) - \bar{a}_4^{earth}(\boldsymbol{I}_z^H I_z^X - \boldsymbol{I}_z^{H'} I_z^X) \quad (3)$$

DOI: 10.1021/acs.jpcb.5b06222
J. Phys. Chem. B 2015, 119, 10035−10041

where the overbar indicates the averaged value of the time dependent coefficients.

Step 2. Nonadiabatic transport of the sample from earth's field to zero field. In the ideal case, the passage is instantaneous and the zero field Hamiltonian ($\mathcal{H}_{zero}$) acts like a sudden perturbation on the steady state density matrix at earth's field ($\bar{\sigma}_{earth}$). The zero field Hamiltonian ($\mathcal{H}_{zero}$) is pure J coupling

$$\begin{aligned}\mathcal{H}_{zero} = &+J_{AA'}(\hat{\boldsymbol{I}}_x^{H}\hat{\boldsymbol{I}}_x^{H'} + \hat{\boldsymbol{I}}_y^{H}\hat{\boldsymbol{I}}_y^{H'} + \hat{\boldsymbol{I}}_z^{H}\hat{\boldsymbol{I}}_z^{H'})\\ &+ J_{AX}(\hat{\boldsymbol{I}}_x^{H}\hat{I}_x^{X} + \hat{\boldsymbol{I}}_y^{H}\hat{I}_y^{X} + \hat{\boldsymbol{I}}_z^{H}\hat{I}_z^{X})\\ &+ J_{A'X}(\hat{\boldsymbol{I}}_x^{H'}\hat{I}_x^{X} + \hat{\boldsymbol{I}}_y^{H'}\hat{I}_y^{X} + \hat{\boldsymbol{I}}_z^{H'}\hat{I}_z^{X})\end{aligned} \quad (4)$$

and the steady state at zero field is

$$\begin{aligned}\bar{\sigma}_{zero} = &\ E/4 + a_3^{zero}(\boldsymbol{I}_x^{H}\boldsymbol{I}_x^{H'} + \boldsymbol{I}_y^{H}\boldsymbol{I}_y^{H'} + \boldsymbol{I}_z^{H}\boldsymbol{I}_z^{H'})\\ &+ a_6^{zero}(\boldsymbol{I}_x^{H}I_x^{X} + \boldsymbol{I}_y^{H}I_y^{X} + \boldsymbol{I}_z^{H}I_z^{X})\\ &+ a_9^{zero}(\boldsymbol{I}_x^{H'}I_x^{X} + \boldsymbol{I}_y^{H'}I_y^{X} + \boldsymbol{I}_z^{H'}I_z^{X})\end{aligned} \quad (5)$$

However, a perfectly diabatic passage cannot be experimentally achieved; therefore, the passage from earth's field to zero was divided in a finite number of intermediate steps (n_{dia}), each of them characterized by its own intermediate field Hamiltonian

$$\begin{aligned}\mathcal{H}_{int}^{(n_{dia})} = &-\nu_H^{(n_{dia})}(\boldsymbol{I}_z^{H} + \boldsymbol{I}_z^{H'}) - \nu_C^{(n_{dia})}I_z^{X}\\ &+ J_{AA'}(\hat{\boldsymbol{I}}_x^{H}\hat{\boldsymbol{I}}_x^{H'} + \hat{\boldsymbol{I}}_y^{H}\hat{\boldsymbol{I}}_y^{H'} + \hat{\boldsymbol{I}}_z^{H}\hat{\boldsymbol{I}}_z^{H'})\\ &+ J_{AX}(\hat{\boldsymbol{I}}_x^{H}\hat{I}_x^{X} + \hat{\boldsymbol{I}}_y^{H}\hat{I}_y^{X} + \hat{\boldsymbol{I}}_z^{H}\hat{I}_z^{X})\\ &+ J_{A'X}(\hat{\boldsymbol{I}}_x^{H'}\hat{I}_x^{X} + \hat{\boldsymbol{I}}_y^{H'}\hat{I}_y^{X} + \hat{\boldsymbol{I}}_z^{H'}\hat{I}_z^{X})\end{aligned} \quad (6)$$

For the implementation of the calculations, see the Supporting Information.

Step 3. Adiabatic transport of the sample from zero to earth's field. According to quantum mechanics, an adiabatic passage is an infinitely slow change of an external condition (in our case of the magnetic field strength), such that the system is allowed to follow continuously the external changes.[32] In the ideal case, the time variation of magnetic field strength (dB_o/dt) or, that is, equivalent, the time variation of proton-carbon frequency difference $d((\nu_H - \nu_C)/dt)$, is infinitely slow and relaxation processes become relevant. In order to find the minimum time for which the remagnetization process is adiabatic, the passage from zero field, where $(\nu_H - \nu_C) = 0$, to the earth's field ($(\nu_H - \nu_C) \approx 1.5$ kHz) was divided into a finite number of steps (n_{adia}), with small variations of $\Delta(\nu_H - \nu_C)$ and a definite Δt delay for each step. For each step, the Hamiltonian is

$$\begin{aligned}\mathcal{H}_{int}^{(n_{adia})} = &-\nu_H^{(n_{adia})}(\boldsymbol{I}_z^{H} + \boldsymbol{I}_z^{H'}) - \nu_C^{(n_{adia})}I_z^{X}\\ &+ J_{AA'}(\hat{\boldsymbol{I}}_x^{H}\hat{\boldsymbol{I}}_x^{H'} + \hat{\boldsymbol{I}}_y^{H}\hat{\boldsymbol{I}}_y^{H'} + \hat{\boldsymbol{I}}_z^{H}\hat{\boldsymbol{I}}_z^{H'})\\ &+ J_{AX}(\hat{\boldsymbol{I}}_x^{H}\hat{I}_x^{X} + \hat{\boldsymbol{I}}_y^{H}\hat{I}_y^{X} + \hat{\boldsymbol{I}}_z^{H}\hat{I}_z^{X})\\ &+ J_{A'X}(\hat{\boldsymbol{I}}_x^{H'}\hat{I}_x^{X} + \hat{\boldsymbol{I}}_y^{H'}\hat{I}_y^{X} + \hat{\boldsymbol{I}}_z^{H'}\hat{I}_z^{X})\end{aligned} \quad (7)$$

EXPERIMENTAL RESULTS AND DISCUSSION

When ethyl acrylate (**1**) was used as hydrogenation substrate, the two parahydrogen protons were added to the acidic moiety, at two to three bonds from the ^{13}C carboxylate atom, while, with vinyl propionate (**3**) the two protons were added at three to four bonds from the target ^{13}C nucleus.

In the first series of hydrogenation experiments, the ^{13}C NMR spectrum was acquired immediately after shaking of the NMR tube, without the application of magnetic field cycling. In these experiments, the ^{13}C carboxylate signal was hyperpolarized only when ethyl acrylate (**1**) was hydrogenated while no polarization was transferred to the ^{13}C carboxylate signal using vinyl propionate (**3**) as hydrogenation substrate (Figure 2).

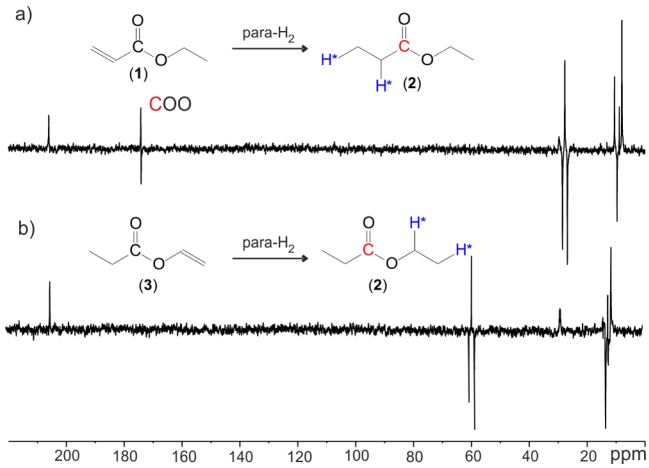

Figure 2. ^{13}C NMR spectra: one scan acquired immediately after hydrogenation with parahydrogen of ethyl acrylate (**1**, spectrum a) and vinyl propionate (**3**, spectrum b), without application of MFC. Hyperpolarized carboxylate signal of ethyl propionate was observed at 174 ppm for substrate **1**, while no polarization was observed using substrate **3**.

In the second series of experiments, magnetic field cycle was applied after hydrogenation with parahydrogen and almost the same hyperpolarization level of the ^{13}C carboxylate signal was observed using both substrates (Figure 3). The enhancement of the signal obtained using 92% enriched parahydrogen was about 2000 ± 200 times compared to the thermal equilibrium at 14.1 T, that corresponds to about 2.3% polarization at this magnetic field.

Calculations of the evolution of the parahydrogen density operator after parahydrogen addition and magnetic field cycling were carried out using the density matrix ($A_3A_2'X$ spin system) and J coupling values reported in Table 1. After parahydrogen addition to the product, without the application of MFC, hyperpolarization was transferred to ^{1}H−^{13}C spin order and hyperpolarized ^{1}H−^{13}C antiphase signals were observed. In Figure 3 are reported the time dependent coefficients of the ^{1}H−^{13}C spin order and ^{1}H−^{1}H coherence (eq 3, coefficients a_4^{earth} and a_1^{earth}). From the averaged values, we obtained that the amount of polarization on ^{1}H−^{13}C spin order ($\bar{a}_4^{earth}$) was about 6 times higher on the hydrogenation product of ethyl acrylate (**1**) than on that of vinyl propionate (**3**) (Figure 4). This was in good agreement with the experimental results and with the fact that polarization transferred to proton−carbon spin order is directly related to ^{1}H−^{13}C J coupling asymmetry.

Magnetic field cycling was then simulated. We assumed, first, that the fast passage from earth's field to zero field was an ideal diabatic passage, infinitely fast, then the zero field Hamiltonian acted as a sudden perturbation of earth's field density operator. Then, after 1 s delay at zero field, the adiabatic remagnetization

DOI: 10.1021/acs.jpcb.5b06222
J. Phys. Chem. B 2015, 119, 10035−10041

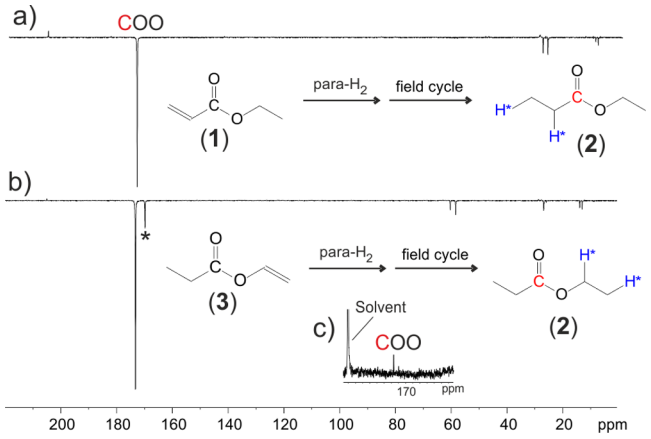

Figure 3. ^{13}C NMR spectra of ethyl propionate obtained from hydrogenation, with parahydrogen, of naturally abundant ^{13}C ethyl acrylate (a) and vinyl propionate (b) following the application of magnetic field cycle. The same hyperpolarization level was observed on the ^{13}C carboxylate signal using both substrates. The asterisk is due to an impurity of the substrate (vinyl acetate). Signal enhancement was obtained from comparison between the S/N of the ^{13}C signal in the hyperpolarized and in the thermally polarized spectra. The thermally polarized spectrum (c) was acquired with 320 scans.

was simulated, with a speed of 50 nT/s. In order to do that, the passage from zero to earth's field was divided into intermediate steps with an increment of 1 Hz of the ^{1}H Larmor frequency ($\Delta\nu_H$) between the steps and a time delay of 500 ms each. We assumed that, under these conditions, the remagnetization passage was adiabatic. From the simulations, the polarization transferred to the heteronuclear net polarization (I_z^C) was about 30% for the acrylate and 35% for the vinyl derivative. The theoretical value obtained for acrylate was in good accordance with the 25−30% polarization experimentally obtained on hydroxyl ethyl propionate.[27] Using this remagnetization rate, the adiabatic passage from zero to earth's field would take 1000s and relaxation phenomena would become relevant, therefore the speed was increased, i.e. the delay for each intermediate step (Δt_{adia}) was reduced. It was found that when the speed was increased to 125 nT/s (Δt_{adia} is reduced to 200 ms), the maximum polarization level was unchanged for both substrates, while when the remagnetization rate was 500 nT/s (Δt_{adia} 50 ms), polarization for the vinyl substrate was reduced to 25%.

From the simulated curves, it was observed that the ^{13}C net magnetization, formed during the adiabatic remagnetization, reached its plateau value at about 1.5 μT (ν_H = 60 Hz). Therefore, the magnetic field range useful for polarization transfer from parahdyrogen spin order to ^{13}C net magnetization is between 0 and 1.5 μT, with the considered substrates. When the remagnetization rate was 500 nT/s, the relevant passage from 0 to 1.5 μT took 3 s (Figure 5, C).

Then, the speed of the first diabatic passage was considered. Since it cannot be infinitely fast, we set the time for this passage, in the simulations, to gradually increasing values. Since the passage from 1.5 μT to zero was not perfectly diabatic, polarization might have been transferred from $^{1}H-^{1}H$ spin order to ^{13}C magnetization in this first step. In particular, it was calculated that, when the first passage took 10 ms, about 1.5% polarization was transferred to ^{13}C net magnetization of the acrylate hydrogenation product and about 10% when the passage took 50 ms. Since relaxation processes at nearly zero magnetic field might lead to fast polarization decay,[34] the first fast passage must preferably take less than 10 ms.

In the end, since obtaining a very low magnetic field, in the order of few nT, is experimentally challenging, a value of the "zero" field was defined. Form calculations, it was obtained that when the low magnetic field limit ("zero field") was 100 nT and ^{1}H Larmor frequency was about 4 Hz, the ^{13}C hyperpolarization obtained at the end of the simulation of MFC was the same as when ν_H was set to zero. In other words, a magnetic field at which the $^{1}H-^{13}C$ frequency difference ($\nu_H - \nu_C$) was equal to their scalar couplings (see Table 1) had the same effect of zero field. Therefore, it was derived that the constrains of magnetic field cycling are between 0.1 and 1.5 μT.

The longitudinal magnetization obtained on protons was also calculated, and it was demonstrated that the net longitudinal magnetization of the sample is zero (Supporting Information).

CONCLUSIONS

The experimental results showed that the polarization transferred from parahydrogen spin order to the ^{13}C carboxylate signal of an ester (ethyl propionate) was the same, when parahydrogen was added both to the acidic (**1**) and to the alcoholic (**3**) moiety, upon application of MFC. It was reported that other polarization transfer methods, based on RF pulse sequences,[24] allow one to obtain higher polarization on ^{13}C net magnetization than MFC; however, it was also shown[35] that the polarization transfer efficiency is directly related with the scalar coupling asymmetry between ^{13}C and the parahydrogen protons. Therefore, these methods would be much less efficient on esters derived from side arm hydrogenation than on other molecules on which parahydrogen protons are added at two to three bonds from the target ^{13}C nucleus. On the contrary, it was demonstrated that MFC is particularly suitable for the hyperpolarization of the ^{13}C carboxylate signals of an ester when parahydrogen is added to the alcoholic moiety and small J

Table 1. Scalar Couplings (Hz) between Parahydrogen Protons and the ^{13}C Carboxylate Nucleus, Relevant for Polarization Transfer[a]

	$^{3}J_{H_AH_B}$	J_{H_AC}	J_{H_BC}	$^{2}J_{H_AH_A}$	$^{2}J_{H_BH_B}$
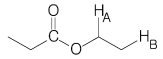	7.5	$^{3}J_{H_AC}$ = 3.2	$^{4}J_{H_BC}$ =1.7	-10.8*	-12.4*
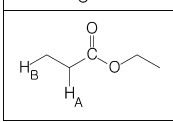	7.5	$^{2}J_{H_AC}$ = -5.6	$^{3}J_{H_BC}$ =7.2	-14.9*	-12.4*

[a]The values with an asterisk were taken from the literature.[33].

DOI: 10.1021/acs.jpcb.5b06222
J. Phys. Chem. B 2015, 119, 10035−10041

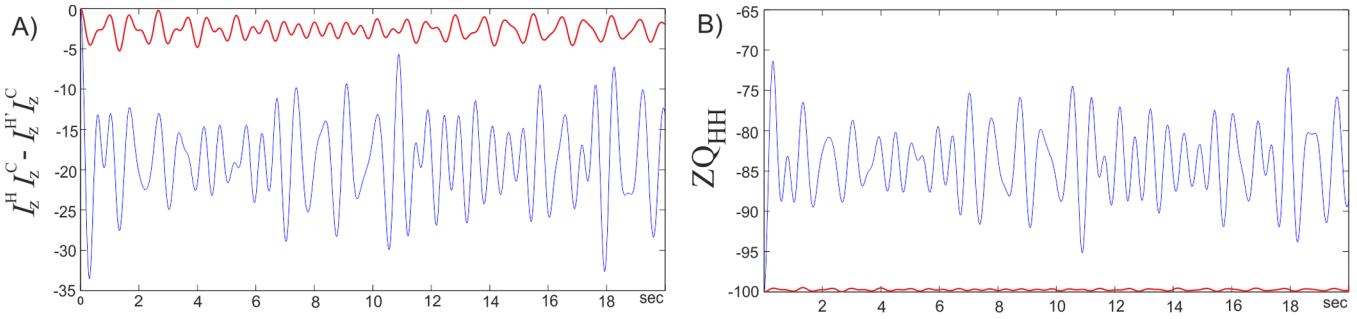

Figure 4. Simulated time-dependent coefficients of $^{1}H-^{13}C$ hyperpolarized spin order (A) and $^{1}H-^{1}H$ zero quantum coherence (B) obtained from the density operator of the $A_3A_2'X$ spin system eq 3 derived from parahydrogen addition, at earth's magnetic field, to vinyl propionate (red) and ethyl acrylate (blue). The averaged value of the theoretical polarization of $^{1}H-^{13}C$ spin order is about 20% using the acrylate substrate (blue) and only about 3% for the vinyl derivative. Almost all polarization is kept on $^{1}H-^{1}H$ zero quantum coherence in the product of vinyl hydrogenation (B, red).

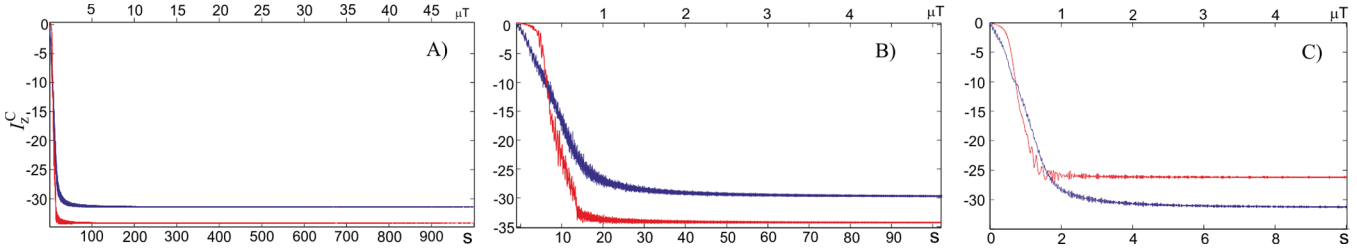

Figure 5. Polarization transferred to ^{13}C net magnetization of the vinyl (red) and acrylate (blue) precursor of ethyl propionate derived from simulation of MFC using the density operator description of parahydrogen. Relaxation processes were not considered. In all these simulations, the first passage was considered perfectly diabatic (infinitely fast), with 1 s evolution at zero field. In panels (A) and (B), the adiabatic remagnetization rate is 25 nT/500 ms (50 nT/s); (B) is merely an enlargement of (A) in which the passage from 0 to 5 μT is shown. In panel (C), the passage from 0 to 5 μT is shown, with adiabatic remagnetization speed 25 nT/50 ms (500nT/s). In this case (C), the passage from 0 to 1 μT takes place in 2 s; maximum polarization on vinyl propionate, hydrogenated with parahydrogen, is now lower than that on ethyl acrylate, on which the maximum polarization is not decreased.

couplings (see Table 1, vinyl propionate derivative) are involved.

It was reported in literature[27] that the application of finely controlled magnetic field cycling allowed one to obtain 25–30% polarization on the ^{13}C carboxylate signal of an acrylate derivative analogous to (**1**). Interestingly, the application of the nonhydrogenative hyperpolarization approach named SABRE (Signal Amplification by Reversible Exchange) at few μT, in a magnetic field shield, allowed, recently, one to obtain about 10% polarization on ^{15}N signal of pyridine and nicotinamide.[36]

Our calculations of the spin states population showed that the maximum polarization that can be obtained is about 30% using both the acrylate (**1**) and the vinyl (**3**) precursors. In order to reach that goal, an accurate control of the speed of the dia/adiabatic passages and of the magnetic field strength must be applied. Furthermore, the high field and low field limits for magnetic field cycle were found, for the considered products, between 1.5 and 0.1 μT. As far as the speed of passages is concerned, the first, fast passage from high to low field must occur in less than 10 ms and the slow remagnetization has to take about 3 s (relaxation phenomena were not considered).

In conclusion, it was stated that an optimized, engineered system for hydrogenation with parahydrogen, such that reported by Hoevener et al.,[37] and for the application of MFC in a controlled way, similarly to that reported by Golman et al.,[27] could reasonably lead to about 25% polarization on ^{13}C carboxylate signals of esters upon parahydrogen addition to the alcoholic part, that is, on SAH derivatives. This polarization level is comparable with that of the [1-^{13}C]-pyruvate currently used for in vivo studies, hyperpolarized by means of DNP.[6,13]

■ ASSOCIATED CONTENT

Supporting Information

Complete Hamiltonian for the $A_3A_2'X$ spin system, Matlab function for the calculation of the density operator time evolution during magnetic field cycling, coefficients of the product operator terms at zero field, and synthesis of hydrogenation substrates. The Supporting Information is available free of charge on the ACS Publications website at DOI: 10.1021/acs.jpcb.5b06222.

■ AUTHOR INFORMATION

Corresponding Author

*E-mail: francesca.reineri@unito.it. Telephone: +39 011 670 6476.

Notes

The authors declare no competing financial interest.

■ ACKNOWLEDGMENTS

Regione Piemonte is gratefully acknowledged for financial support.

■ REFERENCES

(1) Mugler, J. P.; Altes, T. A. Hyperpolarized ^{129}Xe MRI of the Human Lung. *J. Magn.Reson. Imaging* **2013**, *37*, 313–331.

(2) Golman, K.; Axelsson, O.; Johannesson, H.; Mansson, S.; Olofsson, C.; Petersson, J. S. Parahydrogen-Induced Polarization in

Imaging: Subsecond ^{13}C Angiography. *Magn. Reson. Med.* **2001**, *46*, 1−5.
(3) Magnusson, P.; Johansson, E.; Mansson, S.; Petersson, J. S.; Chai, C. M.; Hansson, G.; Axelsson, O.; Golman, K. Passive Catheter Tracking During Interventional MRI Using Hyperpolarized ^{13}C. *Magn. Reson. Med.* **2007**, *57*, 1140−1147.
(4) Golman, K.; in't Zandt, R.; Lerche, M.; Pehrson, R.; Ardenkjaer-Larsen, H. Metabolic Imaging By Hyperpolarized ^{13}C Magnetic Resonance Imaging for in Vivo Tumor Diagnosis. *Cancer Res.* **2006**, *66*, 10855−10860.
(5) Day, S. E.; Kettunen, M. I.; Gallagher, F. A.; Hu, D. E.; Lerche, M.; Wolber, J.; Golman, K.; Ardenkjaer-Larsen, J. H.; Brindle, K. M. Detecting Tumor Response to Treatment Using Hyperpolarized ^{13}C Magnetic Resonance Imaging and Spectroscopy. *Nat. Med.* **2007**, *13*, 1382−1387.
(6) Nelson, S. J.; Kurhanewicz, J.; Vigneron, D. B.; Larson, P. E.; Harzstark, A. L.; Ferrone, M.; van Criekinge, M.; Chang, J. W.; Bok, R.; Park, I. G.; Carvajal, L.; Small, E. J.; Munster, P.; Weinberg, V. K.; Ardenkjaer-Larsen, J. H.; Chen, A. P.; Hurd, R. E.; Odegardstuen, L. I.; Robb, F. J.; Tropp, J.; Murray, J. A. Metabolic Imaging of Patients with Prostate Cancer Using Hyperpolarized [1-^{13}C]Pyruvate. *Sci. Transl. Med.* **2013**, *5*, 198ra108.
(7) Comment, A.; Merritt, M. E. Hyperpolarized Magnetic Resonance as a Sensitive Detector of Metabolic Function. *Biochemistry* **2014**, *53*, 7333−7357.
(8) Kurhanewicz, J.; Vigneron, D. B.; Brindle, K.; Chekmenev, E. Y.; Comment, A.; Cunningham, C. H.; DeBerardinis, R. J.; Green, G. G.; Leach, M. O.; Rajan, S. S.; Rizi, R. R.; Ross, B. D.; Warren, W. S.; Malloy, C. R. Analysis of Cancer Metabolism by Imaging Hyperpolarized Nuclei: Prospects for Translation to Clinical Research. *Neoplasia* **2011**, *13*, 81−97.
(9) Nikolaou, P.; Goodson, B. M.; Chekmenev, E. Y. Nmr Hyperpolarization Techniques for Biomedicine. *Chem. - Eur. J.* **2015**, *21*, 3156−3166.
(10) Ardenkjær-Larsen, J. H.; Fridlund, B.; Gram, A.; Hansson, G.; Hansson, L.; Lerche, M. H.; Servin, R.; Thaning, M.; Golman, K. Increase in Signal-to-Noise Ratio of >10,000 Times in Liquid-State NMR. *Proc. Natl. Acad. Sci. U. S. A.* **2003**, *100*, 10158−10163.
(11) Chekmenev, E. Y.; Hovener, J.; Norton, V. A.; Harris, K.; Batchelder, L. S.; Bhattacharya, P.; Ross, B. D.; Weitekamp, D. P. PASADENA Hyperpolarization Of Succinic Acid for MRI and NMR Spectroscopy. *J. Am. Chem. Soc.* **2008**, *130*, 4212−4213.
(12) Reineri, F.; Viale, A.; Ellena, S.; Boi, T.; Giovenzana, G.; Gobetto, R.; Premkumar, S. S.; Aime, S. N-15 Magnetic Resonance Hyperpolarization via the Reaction of Parahydrogen with ^{15}N-Propargylcholine. *J. Am. Chem. Soc.* **2012**, *134*, 11146−11152.
(13) Nelson, S. J.; Vigneron, D.; Kurhanewicz, J.; Chen, A.; Bok, R.; Hurd, R. DNP-Hyperpolarized ^{13}C Magnetic Resonance Metabolic Imaging for Cancer Applications. *Appl. Magn. Reson.* **2008**, *34*, 533−544.
(14) Witney, T. H.; Kettunen, M. I.; Day, S. E.; Hu, D.; Neves, A. A.; Gallagher, F. A.; Fulton, S. M.; Brindle, K. M. A Comparison Between Radiolabeled Florodeoxyglucose Uptake and Hyperpolarized 13C-Labeled Pyruvate Utilization as Methods for Detecting Tumor Response to Treatment. *Neoplasia* **2009**, *11*, 574−582.
(15) Natterer, J.; Bargon, J. Parahydrogen Induced Polarization. *Prog. Nucl. Magn. Reson. Spectrosc.* **1997**, *31*, 293−315.
(16) Duckett, S. B.; Sleigh, C. J. Applications of the Parahydrogen Phenomenon: a Chemical Perspective. *Prog. Nucl. Magn. Reson. Spectrosc.* **1999**, *34*, 71−92.
(17) Bhattacharya, P.; Chekmenev, E. Y.; Perman, W. H.; Harris, K. C.; Lin, A. P.; Norton, V. A.; Tan, C. T.; Ross, B. D.; Weitekamp, D. P. Towards Hyperpolarized 13C-Succinate Imaging of Brain Cancer. *J. Magn. Reson.* **2007**, *186*, 150−155.
(18) Shchepin, R. V.; Coffey, A. M.; Waddell, K. V.; Chekmenev, E. Y. Parahydrogen Induced Polarization of 1−13C-Phospholactate-d2 for Biomedical Imaging with >30,000,000-fold NMR Signal Enhancement in Water. *Anal. Chem.* **2014**, *86*, 5601−5605.
(19) Zacharias, N. M.; Chan, H. R.; Sailasuta, N.; Ross, B. D.; Bhattacharya, P. Real-Time Molecular Imaging of Tricarboxylic Acid Cycle Metabolism in Vivo by Hyperpolarized 1-C-13 Diethyl Succinate. *J. Am. Chem. Soc.* **2012**, *134*, 934−943.
(20) Bhattacharya, P.; Chekmenev, E. Y.; Reynolds, W. F.; Wagner, S.; Zacharias, N.; Chan, H. R.; Bünger, R.; Ross, B. D. Parahydrogen-Induced Polarization (PHIP) Hyperpolarized Mr Receptor Imaging in Vivo: A Pilot Study of 13c Imaging of Atheroma in Mice. *NMR Biomed.* **2011**, *24*, 1023−1028.
(21) Reineri, F.; Boi, T.; Aime, S. ParaHydrogen Induced Polarization of 13C Carboxylate Resonance in Acetate and Pyruvate. *Nat. Commun.* **2015**, *6*, 5858.
(22) Hurd, R. E.; Yen, Y.-F.; Mayer, D.; Chen, A.; Wilson, D.; Kohler, S.; Bok, R.; Vigneron, D.; Kurhanewicz, J.; Tropp, J.; et al. Metabolic Imaging in the Anesthetized Rat Brain Using Hyperpolarized 1-C-13 Pyruvate and 1-C-13 Ethyl Pyruvate. *Magn. Reson. Med.* **2010**, *63*, 1137−1143.
(23) Goldman, M.; Johannesson, H. Conversion of a Proton Pair Para Order into C-13 Polarization by Rf Irradiation, for Use in Mri. *C. R. Phys.* **2005**, *6*, 575−581.
(24) Goldman, M.; Johannesson, H.; Axelsson, O.; Karlsson, M. Design and Implementation of C-13 Hyperpolarization from Para-Hydrogen, for New MRI Contrast Agents. *C. R. Chim.* **2006**, *9*, 357−363.
(25) Bär, S.; Lange, T.; Leibfritz, D.; Hennig, J.; von Elverfeldt, D.; Hövener, J. B. On the Spin Order Transfer from Parahydrogen to Another Nucleus. *J. Magn. Reson.* **2012**, *225*, 25−35.
(26) Jóhannesson, H.; Axelsson, O.; Karlsson, M. Transfer of Para-Hydrogen Spin Order into Polarization by Diabatic Field Cycling. *C. R. Phys.* **2004**, *5*, 315−324.
(27) Olsson, L. E.; Chai, C. M.; Axelsson, O.; Karlsson, M.; Golman, K.; Petersson, S. MR Coronary Angiography in Pigs With Intraarterial Injections of a Hyperpolarized ^{13}C Substance. *Magn. Reson. Med.* **2006**, *55*, 731−737.
(28) Pravdivtsev, A. V.; Yurkovskaya, A.; Lukzen, N. N.; Ivanov, K. L.; Vieth, H. M. High efficient Polarziation of Spin 1/2 Insensitive NMR Nuclei by Adiabatic Passage Through Level Anticrossing. *J. Phys. Chem. Lett.* **2014**, *5*, 3421−3426.
(29) Barkemeyer, J.; Haake, M.; Bargon, J. Hetro-NMR Enhancement via Parahydrogen Labeling. *J. Am. Chem. Soc.* **1995**, *117*, 2927−2928.
(30) Natterer, J.; Schedletzky, O.; Barkemeyer, J.; Bargon, J.; Glaser, S. J. Investigating Catalytic Processes with Parahydrogen: Evolution of Zero-Quantum Coherence in AA′X Spin Systems. *J. Magn. Reson.* **1998**, *133*, 92−97.
(31) Aime, S.; Gobetto, R.; Reineri, F.; Canet, D. Polarization Transfer from Para-Hydrogen to Heteronuclei: Effect of H/D Substitution. The case of AA′X and $A_2A'_2X$ Spin Systems. *J. Magn. Reson.* **2006**, *178*, 184−192.
(32) Landau, L. D.; Lifshitz, E. M. *Quantum Mechanics*; Pergamon Press: Oxford, 1977.
(33) Barfield, M.; Grant, D. M. The Dependence of Germinal Protons Spin-Spin Coupling Constants on Electron Delocalization in Molecules. *J. Am. Chem. Soc.* **1961**, *83*, 4726−4729.
(34) Reineri, F.; Santelia, D.; Gobetto, R.; Aime, S. Effect of Low and Zero Magnetic Field on the Hyperpolarization Lifetime in Parahydrogenated Perdeuterated Molecules. *J. Magn. Reson.* **2009**, *200*, 15−20.
(35) Cai, C.; Coffey, A. M.; Shchepin, R. V.; Chekmenev, E. Y.; Waddell, K. W. Efficient Transformation of Parahydrogen Spin Order into Heteronuclear Magnetization. *J. Phys. Chem. B* **2013**, *117*, 1219−1224.
(36) Theis, T.; Truong, M. L.; Coffey, A. M.; Shchepin, R. V.; Waddell, K. W.; Shi, F.; Goodson, B. M.; Warren, W. S.; Chekmenev, E. Y. Microtesla Sabre Enables 10% Nitrogen-15 Nuclear Spin Polarization. *J. Am. Chem. Soc.* **2015**, *137*, 1404−1407.
(37) Hoevener, J. B.; Chekmenev, E. Y.; Harris, K. C.; Perman, W. H.; Robertson, L. W.; Ross, B. D.; Bhattacharya, P. PASADENA

DOI: 10.1021/acs.jpcb.5b06222
J. Phys. Chem. B 2015, 119, 10035−10041

Hyperpolarization of ^{13}C Biomolecules: Equipment and Installation. *MAGMA* **2009**, *22*, 111−121.

DOI: 10.1021/acs.jpcb.5b06222
J. Phys. Chem. B 2015, 119, 10035−10041